Sample-Efficient Training of Robotic Guide Using Human Path Prediction Network

Hee-Seung Moon, Jiwon Seo

School of Integrated Technology, Yonsei University, Incheon 21983, Republic of Korea

Abstract

Training a robot that engages with people is challenging, because it is expensive to involve people in a robot training process requiring numerous data samples. This paper proposes a human path prediction network (HPPN) and an evolution strategy-based robot training method using virtual human movements generated by the HPPN, which compensates for this sample inefficiency problem. We applied the proposed method to the training of a robotic guide for visually impaired people, which was designed to collect multimodal human response data and reflect such data when selecting the robot's actions. We collected 1,507 real-world episodes for training the HPPN and then generated over 100,000 virtual episodes for training the robot policy. User test results indicate that our trained robot accurately guides blindfolded participants along a goal path. In addition, by the designed reward to pursue both guidance accuracy and human comfort during the robot policy training process, our robot leads to improved smoothness in human motion while maintaining the accuracy of the guidance. This sample-efficient training method is expected to be widely applicable to all robots and computing machinery that physically interact with humans.

Keywords: Robotic guide, blind navigation, recurrent neural network, evolution strategy, human-robot interaction

Email addresses: hs.moon@yonsei.ac.kr (Hee-Seung Moon), jiwon.seo@yonsei.ac.kr (Jiwon Seo)

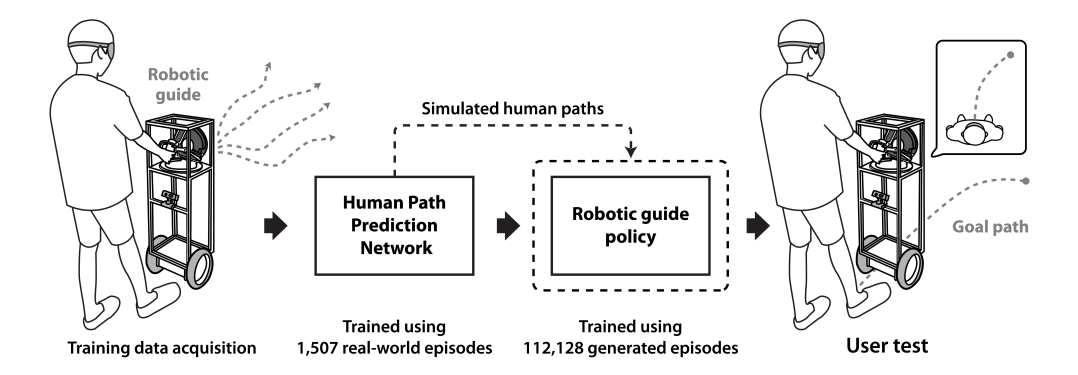


Figure 1: Procedural overview of our training method for a robotic guide. We first train a human path prediction network with a limited number of episodes, and then train the robot policy using numerous virtual episodes generated based on the human path prediction network. The trained robotic guide is validated through a user test to guide users along the given goal path.

1. Introduction

One of the most important advantages that robots provide to human society is complementing the limited sensory abilities of users and providing them with valuable information. The use of a robotic guide, which offers navigational aid to users with a visual impairment, clearly illustrates this benefit. Most people with a visual impairment have difficulty moving freely in an unfamiliar space. In the absence of visual recognition, users can rely on the directional guidance from a robotic guide and achieve a safe route without being disrupted by unknown obstacles. In addition, this type of assistive robot is highly valuable owing to its wide range of uses, including assistance to blind and elderly people who have degraded visuo-motor skills and guidance for people from visually blocked locations, such as during a disaster.

For robots engaging with humans, such as robotic guides and other types of cooperative robots, the ability to understand the user's behavior, i.e., social intelligence, is essential [1, 2, 3]. This allows robots to take more sophisticated movements without reducing their usability and allows users to perceive more credibility from the robots. In particular, when following a robotic guide, the human trajectory is determined differently from person to person, since it depends on a personal gait and a personal reaction of the guidance. Therefore, a robotic guide with such social intelligence can accurately predict a user's movement and guide the user to follow a precise

path. This ensures the safety of blind people even in narrow and crowded places. Furthermore, robot actions based on a user's behavioral model can lead to an increased usability of a robotic guide by inducing smooth user movements and avoiding movements that put stress on the user's muscles, such as during an abrupt turn.

In the past, such social intelligence was provided to the robot through a hand-crafted model [4], however, recent advances in deep-learning-based computing methods may help provide robots with more advanced intelligence. Based on the significant progress made in vision applications and speech recognition using models with a deep neural network structure, neuralnetwork-based methods have been applied to robot manipulation tasks, where the robot operates alone. Traditionally, reinforcement learning (RL) methods, which gradually develop the agent to take an optimal action by providing the degree of success regarding their action, have been exploited to train robots to perform various tasks. In addition, evolution strategy (ES) methods, which find the optimal policy parameters for robots through a black box optimization process, have recently been treated as an alternative approach to the RL methods. By involving a neural network in an RL or ES method, recent studies have demonstrated improved results for training agents in the fields of robot locomotion [5], object grasping [6], emotion recognition [7], game playing [8], and autonomous driving [9].

However, there are critical problems in applying robot training methods in real-world situations, particularly in situations in which humans are required to engage with the robots. The following two major problems are posed. First, considerable amounts of time and spatial resources are required. Although RL and ES methods are effective in finding the optimal action of a robot, they have a sample inefficiency because they require numerous "trial and error" processes. A typical agent training using deep RL methods requires millions of data samples [6, 5], making it practically impossible to collect such a large number of data samples, particularly when an individual should participate with a robot. As a second problem, it is difficult to ensure the safety of the human partner participating in the training process. The robot's movements during the early stage of the RL or ES training period will be unrefined because the robot must go through an "exploration" process of taking various random actions and self-learning by checking the results. Therefore, human involvement in such unpredictable robot movements can cause discomfort to users, or more seriously, lead to a dangerous situation.

In this paper, we present the training method for a robotic guide to solve

the above two problems, which is illustrated in Figure 1. Specifically, the training method is based on our newly proposed human path prediction network (HPPN), which predicts next human movements with regard to robot actions. With our method, people are not involved directly in the robot policy training, and instead we train the HPPN using the movement data of the users following the robotic guide. Our HPPN can generate infinite numbers of virtual human movements. Therefore, our robotic guide can be trained using the ES method through the numerous self-simulations based on the virtual human movements. Our HPPN is trained using only 1,507 movement data, which is a feasible number to collect compared with the number required for an RL or ES training method. In addition, our robot training process is safe because the training dataset for an HPPN is obtained from the general human guidance situation, and all inevitable "trial and error" processes for robot training are enacted only through a virtual simulation.

One more advantage of our training approach is that we can set the training direction of our robotic guide by shaping the reward, which is a numerical score used to assess how well the agent performed. Using infinitely generated data based on an HPPN, various types of intelligence of a robotic guide pursuing different reward functions can be acquired. To demonstrate this, in this study, we train robot polices using two different types of rewards: one that pursues goal efficiency only and another that pursues both the goal efficiency and comfortable movement of the user. In this study, the smoothness of a human motion is used as an evaluation metric to measure the user comfort, which can affect the robot's usability as perceived by its human partner.

To apply the proposed training method, we developed a robotic guide testbed that aims to allow users to efficiently follow along a target path without using their vision. The users consistently receive kinetic guidance from the robot by holding the handle of the haptic device mounted on the robot. In addition, our robotic guide testbed is designed to collect the user's multimodal response data to effectively predict the user's next movement, which is reflected in the robot's next action. To validate our robotic guide and training method, we conducted a user test in an indoor environment using a motion capture system. We verified that the robot effectively guides the user along the goal path based on the user's actual path, and compared the performance of our robot policies trained using the two reward types above with the baseline policy.

1.1. Contributions

The contributions of this paper are summarized as follows:

- We propose a human path prediction network (HPPN) and a training method for robots engaging with human partners based on the HPPN.
 Our training method compensates the two critical problems: the sample inefficiency and human safety problems.
- We develop a robotic guide testbed for blind people that collects multimodal human response data and reflects such data in selecting the robot's action for precise guidance.
- We validate the proposed training method through a user test with eight participants following a trained robotic guide. In addition, we demonstrate that our method is effective in developing human-centered robots by evaluating the smoothness of human motion as well as goalrelated metrics, such as time and accuracy.

2. Related Work

2.1. Robotic Aids for Blind Navigation

Over the last few decades, the need for safe navigation for people with a visual impairment has been continuously raised. Since the pioneering development of robotic aids for blind navigation, such as NavBelt [10] and Guide-Cane [11], robotic assistive technologies have been steadily growing. NavBelt is a belt-typed robotic device equipped with ultrasonic sensors, which provides information regarding the detected obstacles around the user through acoustic feedback. Another type of robotic aid, GuideCane, is a mobile robot moving ahead of the user. Similar to the NavBelt, it detects obstacles through ultrasonic sensors and delivers the kinetic feedback to the user through an attached cane. Subsequent studies on robotic aid have applied various forms of robots using advanced sensors, such as radio-frequency identification [12], laser scanners [12, 13, 14, 3, 15, 16], and depth cameras [17, 3, 18, 19]; however, such devices provide common functionalities, namely, obstacle detection and avoidance [20, 12, 17, 3, 15, 16, 18] and guidance along a given safe path [21, 22].

Recent artificial neural-network-based computing methods have been applied to the robotic guides, contributing especially to robot vision. Regarding

obstacle detection functionality, Poggi and Mattocia [17] developed a wearable device that detects and classifies objects ahead of blind users from depth images using the LeNet model architecture [23] based on a convolutional neural network (CNN). In [24], another wearable device was presented with the aim of assisting the blind users in opening a door. Using a stereo camera, the device detects the position of a doorknob and the hands of the users using a CNN-based model, and delivers audio feedback regarding which direction the users should move their hand. With regard to the function of guidance of a user along a given path, in [21], a robotic guide dog was developed, which recognizes a trail on the floor using a CNN-based deep architecture and determines the next robot motion along the trail.

Despite the need for insight into human movements to guide users in a precise and comfortable manner, such learning-based methods have rarely been applied to analyze a user's movements under the application of a robotic guide. During the blind navigation process, it is a challenge to model human movements accurately because several studies have shown that human movements are affected by several factors, such as the user's acceptance of a navigational aid [25], situational contexts [26], and environmental factors [27]. In [28, 29], researchers developed a behavioral model for users under the guidance of a smartphone and a robotic guide, respectively, using the recurrent neural network (RNN) structures. However, such behavioral models have a limitation in that they are not reflected in practical guidance. For the case of non-learning-based methods, in [3], a robotic guide was developed that detects the user's position using a depth camera and reduces the moving speed to suit the user's intention. However, one limitation is that the user's position data only applies to slowing and lifting the pace, regardless of the guiding path.

Compared to the previous studies that did not properly reflect human behavior to robot actions, our robotic guide uses a neural-network-based model to predict human movements and reflects this prediction data to select the next action of the robot for more precise and comfortable guidance.

2.2. Training of Autonomous Robots

With the development of artificial intelligence technology, there have been significant achievements in training robots to perform complex tasks on their own. RL algorithms have been perceived as a promising way to solve such problems. Researchers have applied recent two popular RL paradigms, an action-value (Q-value)-based approach [30, 31, 32, 33, 34] and a policy

gradient-based approach [35, 36], to real-world robot manipulation tasks, such as object picking [30, 31], door opening [32, 35], and robot locomotion [36]. In addition to RL methods, recent studies have suggested that ES methods can be an effective alternative for robot training [37]. Although ES methods have an even lower sample efficiency than RL methods, ES methods are computationally efficient and have better exploration characteristics, which can provide robustness in robot training. Accordingly, a covariance matrix adaptation evolution strategy (CMA-ES) [38], which is one of the state-of-the-art ES methods, has been applied to robot tasks, such as the locomotion of humanoid [39] and quadruped [40] robots.

As a problem with the RL and ES methods, struggling to collect large amounts of data from real robots, researchers have attempted to acquire training data from the virtual robot movements on a physics-based simulator [35, 41, 42, 36]. These simulator-based approaches have inherent errors between the simulation results and reality; however, researchers have succeeded in mitigating this problem by randomizing the simulation parameters [41] or adapting the parameters through a few real-world rollouts [35].

For the case of robots working with humans, the sample inefficiency problem is still challenging because the collection of training data is more expensive and there are no simulators that fully embody the unpredictable nature of human behavior. Therefore, few studies applied RL or ES methods to train the robots that collaborate with people. In [43], a humanoid robot successfully learned when to extend its hand for a handshake with a human by applying a deep Q-network method. However, the robot had a long training period of 14 days, showing the sample-inefficiency problem. In [44], a data-efficient approach was presented by modeling human interactions based on Gaussian processes. Using the Q-learning method, the researchers trained a robot to cooperatively control the position of a ball on a plank with a human. However, it is hard to say that the human interaction was properly modeled, because only about one minute of operation data by one participant was used for modeling and the evaluation of the trained robot was performed through the same participant.

In this study, we apply the CMA-ES method to train a robotic guide. To solve the sample inefficiency problem above, the proposed HPPN is trained using data obtained from 11 participants to model human movements and produces numerous virtual human movements used in the ES method. Such approach, i.e., modeling an environment with RNN-based structure and using the generated data based on the environment model to train the agent, was

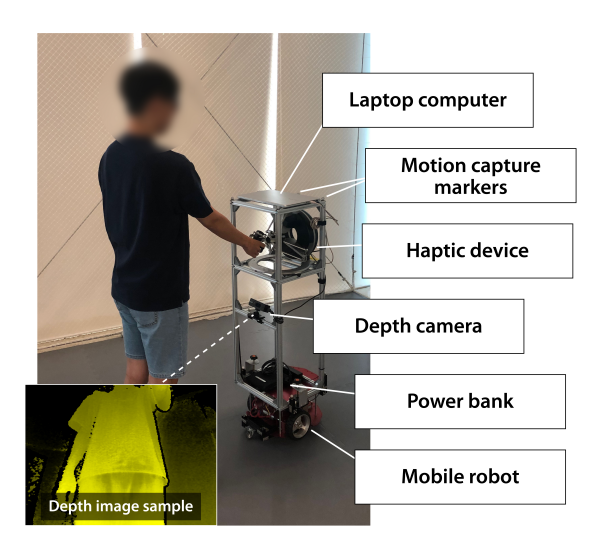


Figure 2: Hardware overview of our robotic guide testbed.

first proposed by Ha and Schmidhuber [45] for training an agent in a gaming environment. Their method, called the World Model, outperformed the state-of-the-art RL methods by utilizing the hidden states of the RNN structure to determine the next action of the agent. We recognized that the World Model method is fully applicable to modeling humans engaging with robots. Therefore, we transform the structure in [45] for use in multimodal human response data from our robotic guide. To the best of our knowledge, this is the first attempt in a real-world human-robot interaction scenario to model human movements regarding the robot's action based on RNNs, and train the robot using the generated episodes from the RNN-based human model.

3. Robotic Guide Testbed

Our robotic guide is designed to guide the user to walk along a goal path by continuously delivering kinetic feedback to the user. Accordingly, as shown in Figure 2, we mounted an Omega.7 haptic device (Force Dimension) on a Stella B2 mobile robot (NTREX, Inc.). To use our robotic guide, the user is instructed to grasp the handle of the haptic device, and therefore the movements of the robot can be transmitted to the user directly through the haptic device. Another issue of our robotic guide design is the acquisition of multimodal human response data according to the robot's movements.

As the first measurement data, a backward-facing Xtion 2 RGB-D camera (ASUS) is mounted on our robotic guide and captures the depth image of the user's torso at a pixel resolution of 640×480 . For the second measurement data, we record the kinetic force input of the user from the haptic device. To quantitatively measure the force exerted on the robot, we apply a spring system that returns more strongly to the origin as the handle of the haptic device moves away from the origin. Specifically, we set the handle to move only in a 2D horizontal plane, and a 2D spring system toward the origin with a spring constant of 500 N/m is implemented in the haptic device. While using the robotic guide, the multimodal human response data are collected every 250 ms, i.e., four times a second. In addition, our robotic guide is equipped with a laptop computer, which controls the mobile robot and the sensors, motion capture markers for precise tracking of robot movements, and a power bank for powering the haptic device.

4. Robot Training Method

4.1. Procedure

Through our robot training procedure, the participants do not directly participate in the robot's RL- or ES-based learning process, which requires numerous data samples and cannot guarantee the safety of the users from the robot's trial-and-error process. Instead, the participants are instructed to follow along various normal movements of our robotic guide, and we train the HPPN using the collected dataset. Among the training dataset, the depth image data have much larger dimensions than the other data types. Therefore, instead of using the depth data directly to train the HPPN, we extract low-dimensional latent feature vectors from the depth images using a variational autoencoder (VAE) [46]. Accordingly, we train the VAE in advance using the depth images in the training dataset, and the HPPN is then trained using robot actions, human haptic data, and compressed depth data as input values. The HPPN can act as a simulator providing the expected human path, given only the action sequence of the robotic guide. Using the HPPN-based simulator, we train the optimal policy parameters for determining the next action of the robotic guide that best meets our goal using the CMA-ES algorithm. To summarize, our training method is applied in the following order:

1. Obtain a dataset of the users following the robot that guides them through various paths.

- 2. Train the VAE using the depth images in the dataset.
- 3. Train the HPPN using the dataset, including the latent feature vectors extracted using the trained VAE.
- 4. On the simulator based on the HPPN, optimize the policy parameters to maximize the cumulative reward of the robotic guide using the CMA-ES algorithm.

4.2. Data Acquisition

We conducted a data acquisition session for training our HPPN. Since it is difficult to invite a sufficient number of blind participants, data were obtained from non-disabled participants with blindfolded, which is also common in previous robotic guide studies in [3, 15, 16]. In this session, 11 participants (2 females and 9 males) between the ages of 20 to 26 years (M = 23.64, SD = 1.67) were involved. All participants were right-handed and had no perception deficiency, including vision or touch abilities. They were informed in advance regarding the purpose of the experiment and were free to rest when needed. During the session, blindfolded participants were instructed to move under the guidance of the robot in an open indoor environment without knowing the path of the robot in advance (Figure 3). In the indoor environment, nine motion capture cameras were installed. Motion capture markers were attached on the robot and the participants; therefore, robot and human path data were collected with mm-level accuracy. Overall, the following time-series data were acquired: i) sets of human and robot movements, i.e., the change of the position and heading angle per timestep, ii) kinetic forces and depth images, measured from the robot sensors and iii) action commands given to the robot, i.e., goal speeds of the left and right wheels, for each timestep.

We aimed at obtaining human data based on as much diverse robot movements as possible, without drastic changes in the robot movements causing discomfort in the participants. To do so, the robot randomly chose its own left and right wheel speeds, but instead of changing the action for each timestep, it set the action to be maintained for arbitrary timesteps. In detail, the rotation speeds of the robot wheels were set between 2.5 to 5 rad/s (0.19 to 0.38 m/s), and the robot retained the action for 4 to 20 timesteps (for 1 to 5 s) before selecting the next action. This method allowed the robot to generate a smooth and diverse guidance route. One episode, which refers to one full guidance of the robot moving with a participant, took an arbitrary time of between 15 and 30 s. During the three-hour experiment, all participants



Figure 3: Experiment setup for training data acquisition. A blindfolded participant follows the robotic guide in an indoor environment with a motion capture system.

were involved in 140 episodes. In total, 1,507 episodes of data were acquired, excluding data in which the robot and human paths were beyond the motion capture range and were therefore not fully measured.

4.3. Human Path Prediction Network

We implemented an HPPN for our robotic guide based on long short-term memory (LSTM) networks [47], an improved variant of an RNN. We extended the structure of the model described in our previous work [29], which was used to predict only the relative position of a person from a robot. Figure 4 (a) shows an overview of our network. Our network employs the following input data: i) robot actions (two-dimensional), ii) kinetic forces applied to the haptic device (two-dimensional), and iii) latent feature vectors of depth images extracted from the pre-trained VAE (16-dimensional). We used the VAE with the structure described in our previous work [48] to compress a depth image with a pixel resolution of 640×480 into a 16-dimensional vector.

Structurally, our network consists of two independent parts. One part is only responsible for the movement of the robot, and the other part is responsible for the movement of the user moving with the robot. The first part (left side of Figure 4 (a)) uses the robot's action only as an input, and outputs the next robot movement, i.e., the change of the position and heading per timestep, using two layers of the LSTM, which have eight hidden units each. Unlike the first part, which only deals with robot-related data, the second part (right side of Figure 4 (a)) focuses on predicting human motion using both the robot action and the human response, namely the kinetic

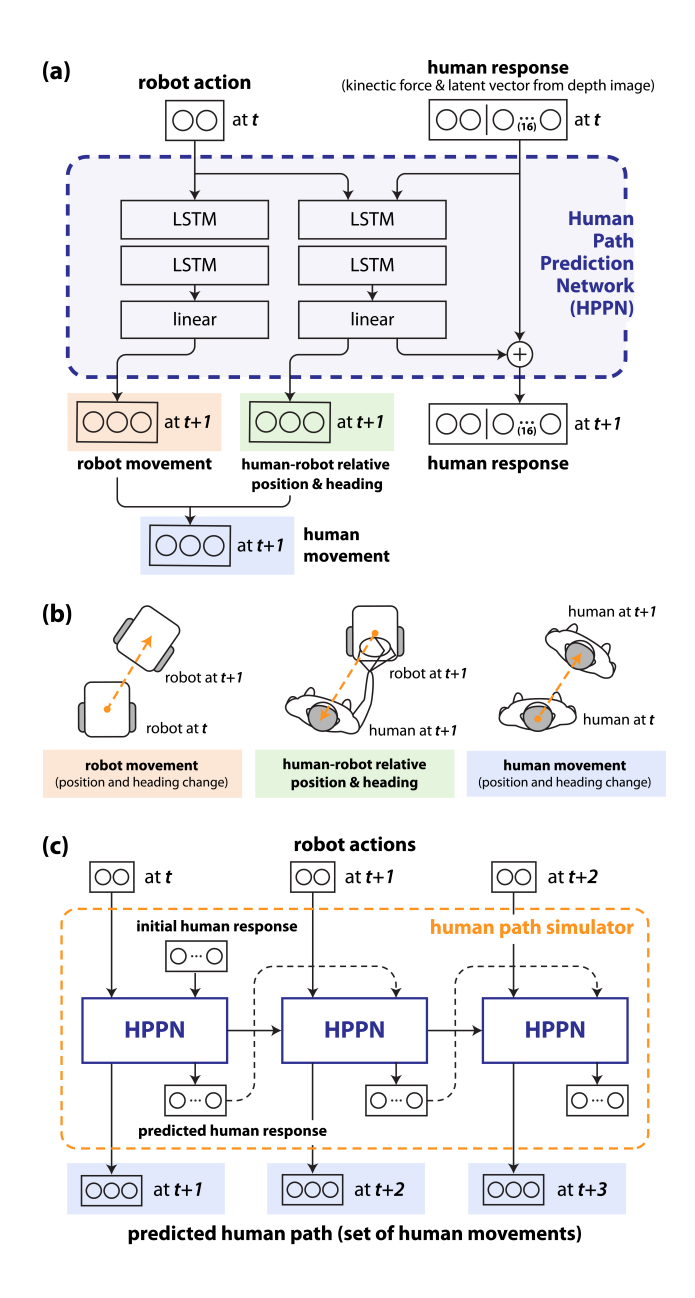


Figure 4: (a) Overview of our HPPN. The number of the circles in the box represents the size of each data. (b) Schematic representations robot movement, human-robot relative position and heading, and human movement. (c) The use of an HPPN as a simulator. The expected human path can be obtained by inputting the sequence of the robot actions.

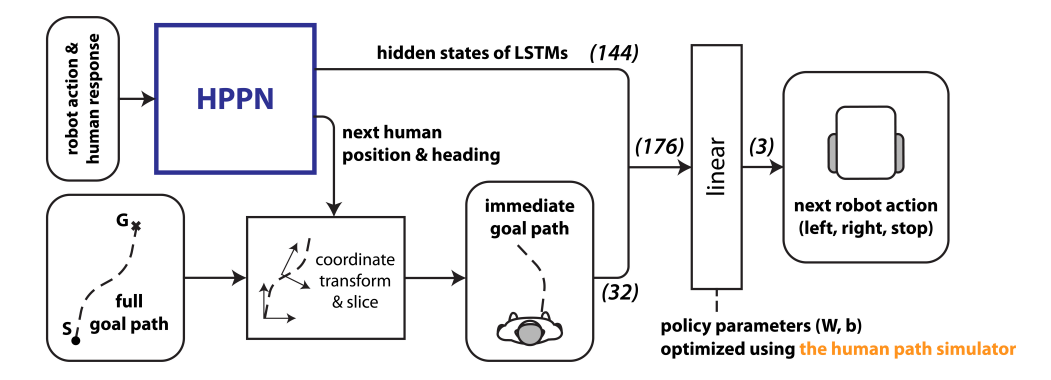


Figure 5: Process by which our robotic guide determines the next action according to the input data (current action, human response and goal path) and the policy parameters optimized using the human path simulator in Figure 4 (c). The numbers in parentheses indicate the dimensions of each data.

force and latent vector from the depth image. Two layers of LSTMs with 64 hidden units are used to predict the human-robot relative position and heading at the next timestep. The network also predicts the next human response to create a simulator that predicts human movements using only the robot actions, as shown in Figure 4 (c), by applying a structure that uses the predicted human response as a new input for the next timestep. We applied a residual connection between the human response input and output, and therefore the network only predicts the amount of change, thus enabling more stable training. By obtaining robot movements in the first part and human-robot relative positions and headings in the second part, we acquire the predicted human movements as timestep progresses.

In detail, we used approximately 130K depth images in the training dataset to train the VAE, which was trained for 200 epochs using an Adam optimizer (learning rate of 0.001). For the HPPN, we trained the dual structures independently. By windowing the data with a size of 20 timesteps (i.e., 5 s), approximately 100K time sequential data samples were used to train the HPPN. Using the Adam optimizer at a learning rate of 0.01, the robot-and human-related LSTM structures were trained for 500 and 80 epochs, respectively.

4.4. Training of Robotic Guide on Simulator

We applied the CMA-ES method to train a robot policy with the generated episodes based on the human path simulator. The CMA-ES method is

an evolutionary optimization algorithm that finds a solution that maximizes the objective function of a particular problem. During every generation, the method performs episodes with a population size of the candidate solutions and develops candidate solutions in a way that yields a better objective function over a generation. We implemented our robot policy using parameters that can be optimized using the CMA-ES method and defined rewards for the robot that can be used as the objective function, as described in the following sections. Using the human path simulator, a human path when the robot moves based on the current policy with the given parameters can be predicted. Under the CMA-ES method, the policy parameters improve using the reward calculated from the predicted human path, and this process is repeated to find the optimal policy parameters.

4.4.1. Robot Policy

During every timestep, our robotic guide determines the action to take in the next timestep by passing a robot's current feature vector through a single linear layer as follows:

$$(next\ robot\ action) = W \cdot (feature\ vector) + b,$$

where W and b represent the weight and bias of the linear layer, and are the policy parameters optimized through the CMA-ES. The feature vector of the robot consists of two major features, as shown in Figure 5. First, to contain the motion information of the user and the robot over time, we used the hidden state values of the LSTMs in the HPPN at the current timestep. Because the LSTMs were designed to predict the next human movement and affected by the sequential input data (robot actions and human responses), the hidden states of the LSTMs will integrate this information and are useful to reflect it in the robot's next action. Second, the information of the goal path that the user should walk along is provided to the robot to determine the next action. Instead of using a full goal path directly, only the immediate goal path for the current timestep is employed as the timestep passes. For this purpose, the coordinate transformation and slicing processes are performed at every timestep based on the predicted human position and heading obtained from the HPPN.

The feature vector we used has a size of 176, which is obtained by flattening the hidden state values of the LSTMs with a size of 144 (2 \times 8 hidden units + 2 \times 64 hidden units) and the immediate goal path data consisting of

16 two-dimensional points. The robot action determined through the policy consists of three dimensions: the left motor speed, right motor speed, and degree ranging from 0 to 1 to determine whether to stop (the robot stops if the degree is over 0.5). Accordingly, our policy parameter has a size of 531, including a weight matrix with a size of 3×176 and a three-dimensional bias vector.

4.4.2. Reward

In this study, we set up two reward types: i) a reward that only considers goal efficiency (referred to as G Only) and ii) a reward that also considers how the robot comfortably guides the user in addition to the goal efficiency (referred to as G + H). In detail, the cumulative rewards of an episode based on these two reward types were calculated as follows:

• G Only: This reward is determined based on the metrics related only to the goal efficiency, i.e., the completion time and accuracy. As a metric to measure the level of accuracy, the Fréchet distance, which calculates the similarity between two paths, was used to indicate how accurately the user actually moved along the goal path. The total calculation formula is as follows:

```
(cumulative\ reward) = -1 \times (completion\ time)
-100 \times (Fr\'{e}chet\ distance).
```

In addition, if the completion time exceeded the maximum timestep (which we set to 100 timesteps), the episode was terminated and a penalty of -500 was given.

• G + H: In addition to the metrics used for G Only, we applied human motion smoothness to consider the comfort of the user. As a quantitative measure of the motion smoothness, we used the spectral arc length [49]. The calculation formula is as follows:

```
(cumulative\ reward) = -1 \times (completion\ time)
-100 \times (Fr\'{e}chet\ distance)
+30 \times (spectral\ arc\ length\ of\ human\ path).
```

By setting up two different rewards as above and testing them through user experiments, we indicated the following two aspects. First, our trained

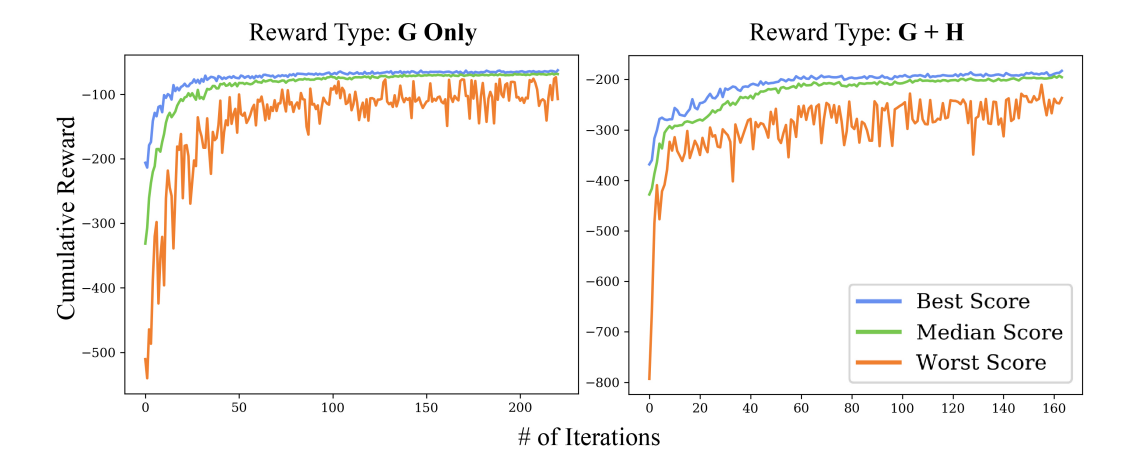


Figure 6: Convergence of the cumulative reward of our robot policy trained using the CMA-ES method with the G Only (left) and G + H (right) type rewards.

HPPN have the advantage of training numerous robot policies with various characteristics by utilizing the fact that the simulator based on the HPPN can generate countless virtual human paths. Second, observing the actual performance of the two robot policies trained using the G + H reward, which considers human convenience, and the G Only reward, which does not, the generated episodes based on the HPPN can be deemed sufficiently effective for the development of real-world human-centered robots.

4.4.3. Implementation Details

For the CMA-ES method, we set 32 population sizes for each generation, which means that 32 different policy parameters were tested using the virtual simulations from one generation. For each policy parameter, we simulated 16 episodes based on 16 randomly generated goal paths of 4 m in length, and collected their average cumulative rewards. Figure 6 shows the robot policy training results for each reward type using this CMA-ES method. As a result of training applied until the objective functions of the best performer converged, it took 219 generations for G Only, and 163 generations for G + H. These figures indicate that 112,128 virtual episodes (219 × 32 × 16) were conducted for G Only, and 83,456 (163 × 32 × 16) were conducted for G + H. Considering that only 1,507 episodes were actually collected, our training method shows that the ES approach can be applied with a notably better

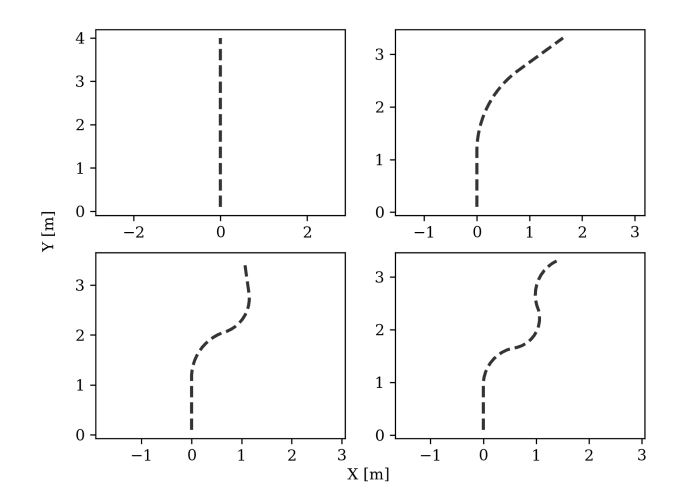


Figure 7: Goal paths used for the user test. All paths are 4 m long and created by adjusting the number of curvatures from zero to three. By laterally inverting the goal paths except for the straight line, seven goal paths were used for the user test.

sample efficiency.

5. User Test

We conducted a user test to validate our robotic guide trained with the two reward types mentioned above. Eight participants (1 female and 7 males) between 24 to 29 years of age (M=25.75, SD=1.48) were involved in the user test. None of them participated in the training data acquisition session, and all were right-handed and had no perception deficiency. Similar to the preceding training session, each participant was blindfolded and instructed to follow the robot's guidance without knowing the path information. Using the motion capture system, the precise path data of the participants were collected with mm-level accuracy and employed to analyze the performance of our robotic guide. Note that the motion capture system that generated the ground truth was used only for the evaluation purpose during the user test. The trained robot does not utilize any information from the motion capture system when guiding the user.

While the robot was set to take randomly generated movements during the training session, the trained robot policies were applied to guide the participants to follow the goal path during this user test. To investigate

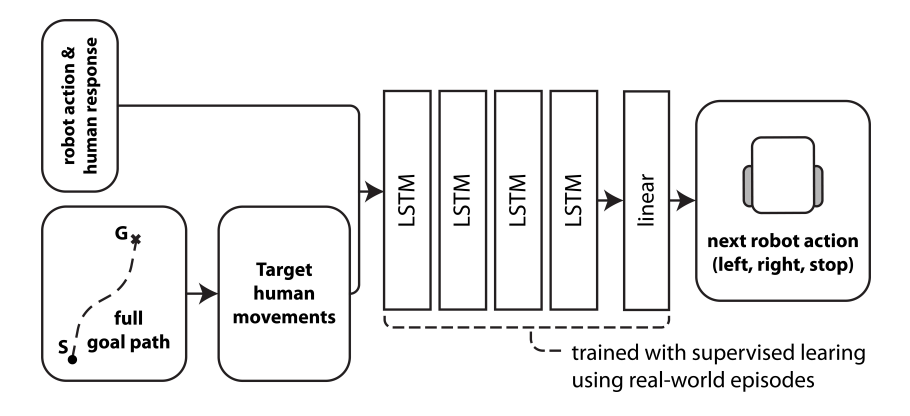


Figure 8: Overview of the baseline policy network.

the performance of the robotic guide according to the path complexity, we generated various goal paths, controlling the number of curvatures in the path. As depicted in Figure 7, we constructed 4 m long goal paths with zero to three curvatures. By laterally inverting the three goal paths except for the straight line, seven goal paths were used for the user test.

In this user test, three robot policies were evaluated: a baseline policy, described below, and our two robot policies trained using the G Only and G + H rewards. All participants conducted three episode trials for each of the 21 pairs of robot policy-goal path. Accordingly, each participant of this user test performed 63 episodes (7 goal paths \times 3 robot policies \times 3 trials) during a 1.5 h long experiment. Because the order of each robot policy-goal path pair was determined randomly, the participants were unable to know what conditions they were currently being guided under.

5.1. Baseline Policy

As a baseline policy, we developed a neural-network-based model that directly outputs the robot's next action from input data, which is the best way to train a robot with a limited amount of data and has shown effective performance in recent studies [21, 50]. As mentioned earlier, the conventional RL and ES methods suffer from the sample inefficiency problem. Thus, it is evident that the training with those methods will not be completed using the very limited number of real-world data samples used in this study. Therefore, a neural-network-based model, which can be trained using supervised learning even with the limited dataset we acquired, is implemented as

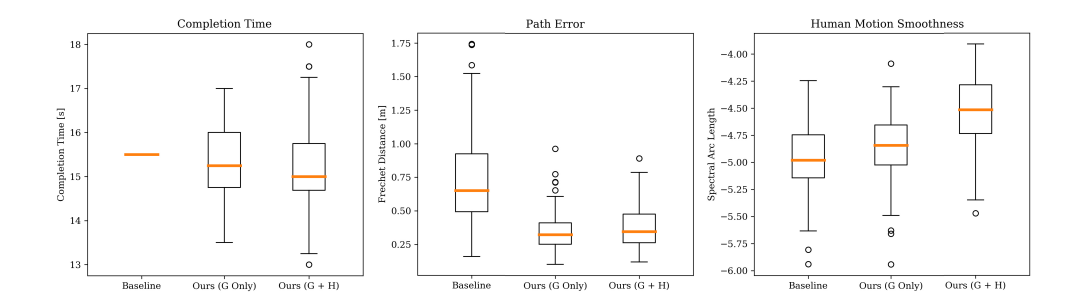


Figure 9: Box plot showing the overall performance results of each robot policy.

our baseline policy. The performance of our training method based on the proposed HPPN was compared with that of the baseline policy.

The baseline policy network consists of four LSTMs with eight hidden units, as shown in Figure 8. The network has the same input (current robot action, human response, and goal path) and output (next robot action) data as the robot policy we presented in Figure 5. Because the training dataset consists of the actual distances that a person moved rather than a goal path, we delivered the goal path information in the form of target human movements that the robot should guide. Accordingly, an additional process that converts a given goal path into plausible target human movements is required for the user test. For the processing, we set the target speed of the user to 0.36 m/s, which corresponds to the top 80% of the distribution of human speeds obtained from the training dataset.

6. Results

We evaluated the performance of the robotic guide from two perspectives: goal efficiency and user comfort. In terms of the goal efficiency, the completion time and path error were used as the evaluation metrics. The completion time of the robot guidance was measured as the time taken from the start to the stop of the robot. To quantify the path error, the Fréchet distance between the goal path and the actual path of the user was measured. For the user comfort, we focused on how comfortable the user could move under the guidance of the robot. A smooth movement of a person has been identified as the result of minimized effort [51, 52]. Therefore, we utilized the spectral arc length to measure the smoothness of the human movements.

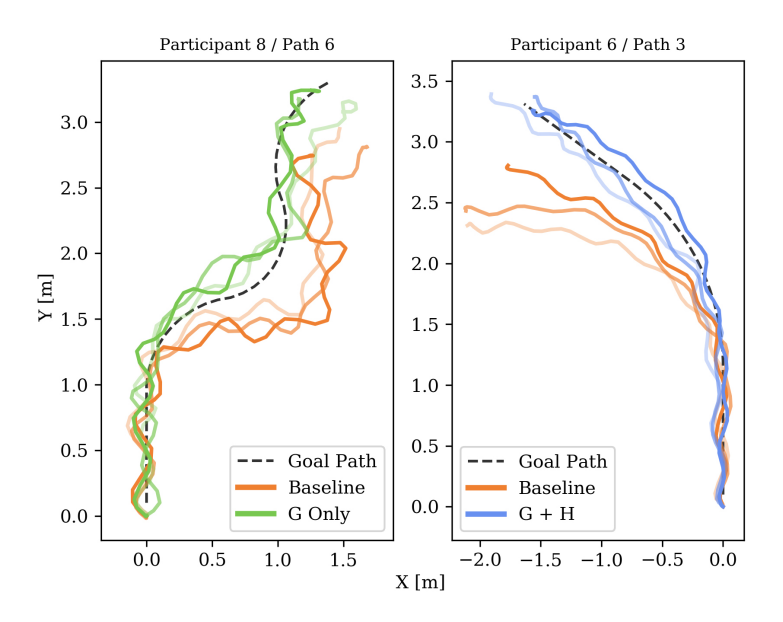


Figure 10: Samples of the user's actual path following the robot with the baseline policy and the G Only (left) and G + H (right) type policies. User paths during different trials are distinguished by the line transparency.

Figure 9 shows box plots of the distributions of the above three metrics measured during all episodes of the user test. Through the paired t-test (eight participants), we verified whether one policy led to a significant difference in the guidance performance over another. In terms of the completion time, all three robot policies required a similar amount of time to guide the users. Note that, during the user test applying the same goal path length, the baseline policy consistently resulted in the same completion time. Because a fixed target user speed was utilized for the baseline policy, a fixed-length input data sequence was provided to the robot. Therefore, the robot with the baseline policy ended the guidance after the same amount of time. In terms of the path error, both the G Only and G + H type robot policies induced significant decrease of path error compared to the baseline policy (t = 9.931,p < 0.001 and t = 8.478, p < 0.001, respectively). No significant differences were found between the G Only and G + H type robot policy (t = 1.361, p = 0.216). In terms of the smoothness of the human motion, the results of the G + H type policy significantly outperformed those of both the G Only type policy (t = 8.236, p < 0.001) and the baseline policy (t = 12.975, p < 0.001), whereas the G Only type policy and the baseline policy did not show a significant difference (t = 2.175, p = 0.066). This indicates that our robot policy training method considering the motion smoothness is sufficiently effective in inducing smooth movements of a real person.

Figure 10 shows samples of the user's actual path when following the robot using the baseline policy and that of our robot policies (G Only and G + H), which were collected during three trials conducted along the same goal path. It is clearly shown that the user's path is closer to the dotted goal path, when using our robot policies. The oscillatory behavior of the user is a natural response to stepping on the left and right foot and is also described in [53]. The trajectory of the robot does not have this oscillation, which will be shown in Figure 11.

6.1. How the Robot Adequately Guides Different Users

Our robotic guide was designed to reflect human multimodal response data to better guide people to a goal path at each timestep. In other words, the robot learns to recognize the user's behavioral patterns and chooses the best action based on the expected path of the user. We examined episodes from the user test to see how our robotic guide adequately guides different users.

Figure 11 shows the path samples of the robots and humans during episodes in which the G Only type robot policy guided two different participants to the same goal path. In Figure 11 (a), participants 1 and 6 showed different behavioral patterns in following the robot. Participant 1 tended to walk on the right side of the robot ahead, whereas participant 6 tended to walk on the left (as illustrated in the circle). Accordingly, our robotic guide showed different path movements for each participant. When guiding participant 1, the robot led to the left side of the goal path, and when guiding participant 6, the robot led to the right side of the goal path, consequently guiding the users closer to the goal path. These movements of the robot also appeared in another episode (Figure 11 (b)). While guiding along the same goal path, participant 2 walked along the left side of the robot, and participant 5 followed almost the same path as the robot. Accordingly, the different guidance paths of the robot were observed, moving toward the right side of the goal for participant 2, and moving as close as possible toward the goal path for participant 5. These episodes show that our

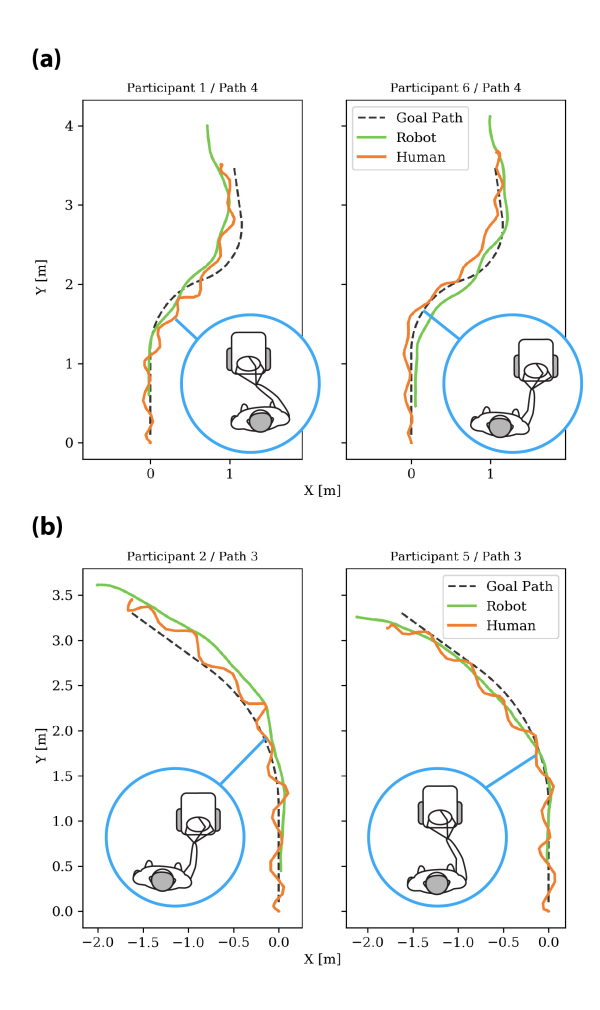


Figure 11: Path samples of the robot using the G Only policy when moving differently for different participants for the same goal path. The illustrations in the circle depict which side the users are on when following the robot for each path.

trained robot effectively learned the different behavioral patterns of humans and chose adequate actions for different users.

6.2. How the Robot Comfortably Guides Users

During this user test, the G + H type robot policy showed a superior smoothness of the human motion compared to the baseline and G Only type policies. We further analyzed how the G + H type policy, which was trained on virtual simulations, improved the motion smoothness of the actual users.

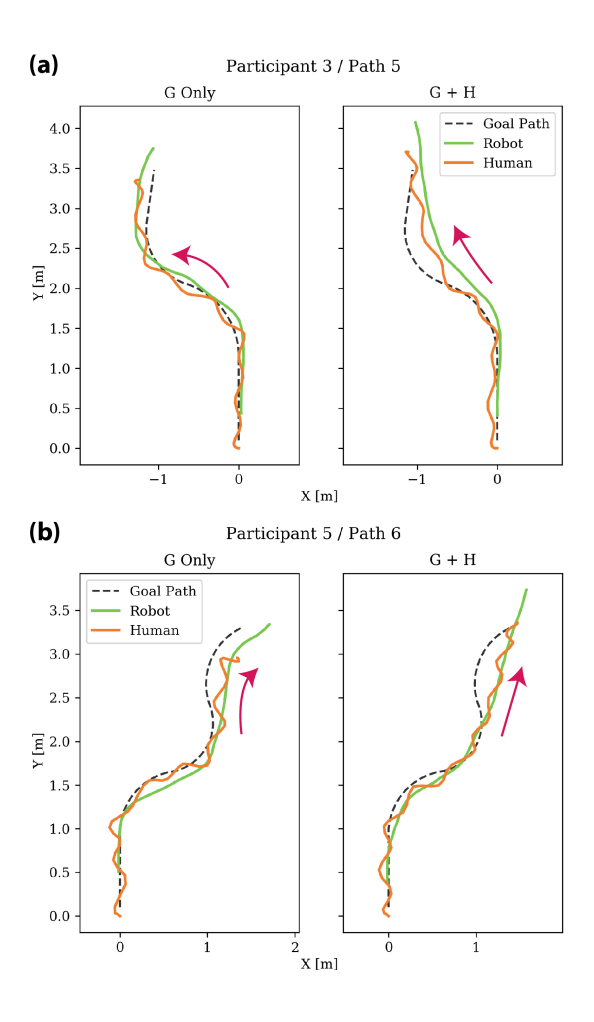


Figure 12: Path samples showing how robots under the G Only and G + H type policies behave differently for the same participant and the same goal path.

Our analysis proceeded in two ways, in terms of the actual guiding path and the change in speed of the robot.

First, we compared the actual robot paths generated by the G Only and G + H type robot policies for the same participants based on the two path samples in Figure 12. In both path samples, we observed that the G + H type robot gave up turning sharply and chose a less convoluted path, although a sharp turn was required to follow the sharply turning goal path. In Figure 12 (a), the G + H type robot rotated only slightly along the goal path, whereas the G Only type robot rotated obviously toward the left along

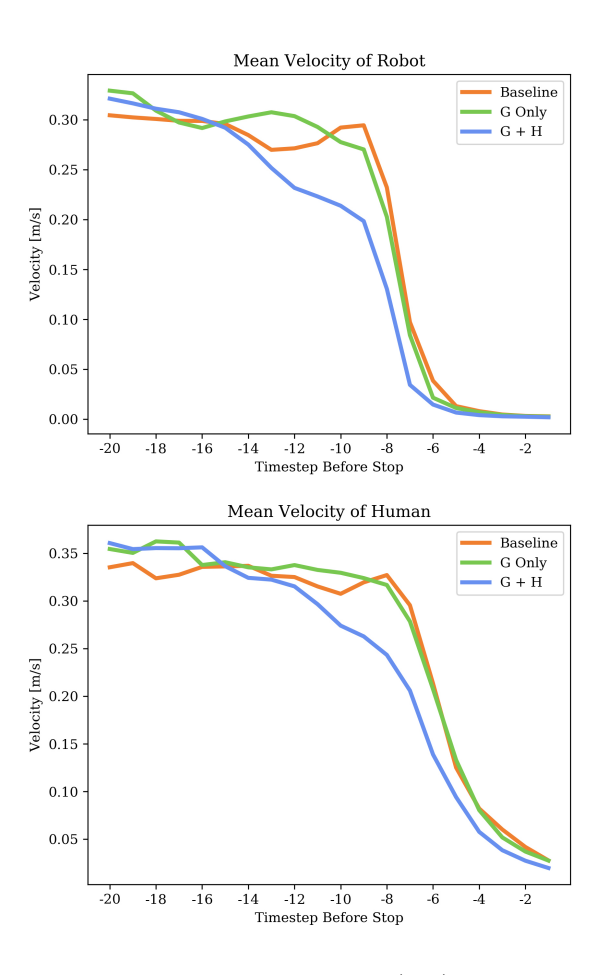


Figure 13: The mean velocity changes of the robot (top) and the user (bottom) before the robot stops.

the goal path (as depicted by the red arrows). In addition, in Figure 12 (b), the G+H type robot gave up the last turn and went straight, whereas the G Only type robot moved along the goal path to the end (as depicted by the red arrows). These examples demonstrate that the G+H type policy learned to avoid sharp rotations that can lower the smoothness of the human motion, even if a certain level of accuracy is lost. However, such movements of the G+H type robot that noticeably reduce accuracy as in Figure 12 were rarely observed and, as shown in Figure 9, did not significantly reduce guidance accuracy compared to the G Only type robot in general.

For the second aspect, we analyzed for all three policies the mean velocities of the robot and the user for 20 timesteps (i.e., 5 s) before the robot stopped, as shown in Figure 13. The analysis showed that there were no noticeable differences between the baseline and G Only type policy; however, the G+H type robot started decelerating earlier than the other two policies, and gradually slowed down. The other two policies started the deceleration of the robot at 8 to 10 timesteps prior to stopping, whereas the G+H type policy started the deceleration at 12 to 14 timesteps before it stopped. Accordingly, the speed of the user following the robot also decreased early and slowly under the G+H type policy as compared to the other two policies. Consequently, this change in speed demonstrates that the G+H type policy increased the smoothness of the human motion by learning its own gradual slowdown process prior to stopping.

7. Conclusion

In this paper, we presented the HPPN, a neural network model that predicts next human movements with regard to robot actions, and the training method based on the HPPN for robots that engage with human partners. Our approach is valuable in that it can solve the sample inefficiency and human safety issues raised when training robots that move with people. Applying our training method to the development of a robotic guide for those with a visual impairment, we collected 1,507 real-world episodes, and then generated more than 100,000 virtual episodes for the robot policy training. The results of a user test indicate that our method is effective in training robots to increase the guidance accuracy compared to the baseline method. In addition, using our method, the robot learned how to provide adequate guidance according to the human behavioral pattern and how to guide the user comfortably. Currently, our robot estimates its own location based only on the robot action commands used. If additional sensors are used to increase the localization performance, more accurate guidance will be possible over longer distances.

The proposed method is widely applicable to all robots and computing machinery that physically interact with humans. In addition, our research suggests an effective way of developing a human-centered robot. One of the remarkable points of our work is that, by the reward shaping that considers human comfort during the policy training process, our robot leads to an improved smoothness in human motion without significant degradation in the

guidance accuracy, as demonstrated during the user test. We envision that our sample-efficient training method, which allows robot to learn both goal efficiency and social intelligence based on the human model, will contribute to the field of human-robot interaction.

Acknowledgements

This work was supported by the Basic Science Research Program through the National Research Foundation of Korea (NRF) funded by the Ministry of Education (NRF-2018R1D1A1B07043580).

References

- [1] S. Soyguder, Intelligent control based on wavelet decomposition and neural network for predicting of human trajectories with a novel vision-based robotic, Expert Syst. Appl. 38 (11) (2011) 13994–14000.
- [2] K. Charalampous, I. Kostavelis, A. Gasteratos, Robot navigation in large-scale social maps: An action recognition approach, Expert Syst. Appl. 66 (2016) 261–273.
- [3] S. Scheggi, M. Aggravi, D. Prattichizzo, Cooperative navigation for mixed human–robot teams using haptic feedback, IEEE Trans. Human–Mach. Syst. 47 (4) (2016) 462–473.
- [4] D. Helbing, P. Molnar, Social force model for pedestrian dynamics, Phys. Rev. E 51 (5) (1995) 4282–4286.
- [5] X. B. Peng, G. Berseth, M. Van de Panne, Terrain-adaptive locomotion skills using deep reinforcement learning, ACM Trans. Graph. 35 (4) (2016) 81.
- [6] S. Levine, P. Pastor, A. Krizhevsky, J. Ibarz, D. Quillen, Learning handeye coordination for robotic grasping with deep learning and large-scale data collection, Int. J. Robot. Res. 37 (4-5) (2018) 421–436.
- [7] L.-A. Perez-Gaspar, S.-O. Caballero-Morales, F. Trujillo-Romero, Multimodal emotion recognition with evolutionary computation for human-robot interaction, Expert Syst. Appl. 66 (2016) 42–61.

- [8] V. Mnih, K. Kavukcuoglu, D. Silver, A. A. Rusu, J. Veness, M. G. Bellemare, A. Graves, M. Riedmiller, A. K. Fidjeland, G. Ostrovski, et al., Human-level control through deep reinforcement learning, Nature 518 (7540) (2015) 529–533.
- [9] R. Hadsell, A. Erkan, P. Sermanet, M. Scoffier, U. Muller, Y. LeCun, Deep belief net learning in a long-range vision system for autonomous off-road driving, in: Proc. IEEE/RSJ Int. Conf. Intell. Robot. Syst., 2008, pp. 628–633.
- [10] S. Shoval, J. Borenstein, Y. Koren, The navbelt-a computerized travel aid for the blind based on mobile robotics technology, IEEE Trans. Biomed. Eng. 45 (11) (1998) 1376–1386.
- [11] I. Ulrich, J. Borenstein, The guidecane-applying mobile robot technologies to assist the visually impaired, IEEE Trans. Syst., Man, Cybern. A 31 (2) (2001) 131–136.
- [12] V. Kulyukin, C. Gharpure, J. Nicholson, G. Osborne, Robot-assisted wayfinding for the visually impaired in structured indoor environments, Auton. Robot. 21 (1) (2006) 29–41.
- [13] J. H. Kim, I. Bae, C.-H. Quan, S. H. Lee, P. W. Son, J. H. Rhee, S. Kim, J. Seo, Collaborative navigation of uav and ugv using vision and lidar sensors, in: ION Pacific PNT Conference, 2013.
- [14] J. H. Kim, J.-W. Kwon, J. Seo, Multi-uav-based stereo vision system without gps for ground obstacle mapping to assist path planning of ugv, Electronics Letters 50 (20) (2014) 1431–1432.
- [15] A. Wachaja, P. Agarwal, M. Zink, M. R. Adame, K. Möller, W. Burgard, Navigating blind people with walking impairments using a smart walker, Auton. Robot. 41 (3) (2017) 555–573.
- [16] Z. Li, R. Hollis, Toward a ballbot for physically leading people: A human-centered approach, in: Proc. IEEE/RSJ Int. Conf. Intell. Robot. Syst., IEEE, 2019, pp. 4827–4833.
- [17] M. Poggi, S. Mattoccia, A wearable mobility aid for the visually impaired based on embedded 3d vision and deep learning, in: Proc. IEEE Symp. Comput. Commun., 2016, pp. 208–213.

- [18] H.-C. Wang, R. K. Katzschmann, S. Teng, B. Araki, L. Giarré, D. Rus, Enabling independent navigation for visually impaired people through a wearable vision-based feedback system, in: Proc. IEEE Int. Conf. Robot. Autom., 2017, pp. 6533–6540.
- [19] S. Kayukawa, K. Higuchi, J. Guerreiro, S. Morishima, Y. Sato, K. Kitani, C. Asakawa, Bbeep: A sonic collision avoidance system for blind travellers and nearby pedestrians, in: Proc. CHI Conf. Hum. Factors Comput. Syst., 2019, pp. 1–12.
- [20] M. Bousbia-Salah, M. Bettayeb, A. Larbi, A navigation aid for blind people, J. Intell. Robot. Syst. 64 (3-4) (2011) 387–400.
- [21] T.-K. Chuang, N.-C. Lin, J.-S. Chen, C.-H. Hung, Y.-W. Huang, C. Tengl, H. Huang, L.-F. Yu, L. Giarré, H.-C. Wang, Deep trail-following robotic guide dog in pedestrian environments for people who are blind and visually impaired-learning from virtual and real worlds, in: Proc. IEEE Int. Conf. Robot. Autom., 2018, pp. 1–7.
- [22] A. Ghosh, J. Penders, P. E. Jones, H. Reed, Experience of using a haptic interface to follow a robot without visual feedback, in: Proc. IEEE Int. Symp. Robot. Hum. Interact. Commun., 2014, pp. 329–334.
- [23] Y. LeCun, L. Bottou, Y. Bengio, P. Haffner, et al., Gradient-based learning applied to document recognition, Proc. IEEE 86 (11) (1998) 2278–2324.
- [24] L. Niu, C. Qian, J.-R. Rizzo, T. Hudson, Z. Li, S. Enright, E. Sperling, K. Conti, E. Wong, Y. Fang, A wearable assistive technology for the visually impaired with door knob detection and real-time feedback for hand-to-handle manipulation, in: Proc. IEEE Int. Conf. Comput. Vision, 2017, pp. 1500–1508.
- [25] A. Abdolrahmani, W. Easley, M. Williams, S. Branham, A. Hurst, Embracing errors: Examining how context of use impacts blind individuals' acceptance of navigation aid errors, in: Proc. CHI Conf. Hum. Factors Comput. Syst., 2017, pp. 4158–4169.
- [26] J. Guerreiro, E. Ohn-Bar, D. Ahmetovic, K. Kitani, C. Asakawa, How context and user behavior affect indoor navigation assistance for blind people, in: Proc. Web for All Conf., 2018, p. 2.

- [27] H. Kacorri, E. Ohn-Bar, K. M. Kitani, C. Asakawa, Environmental factors in indoor navigation based on real-world trajectories of blind users, in: Proc. CHI Conf. Hum. Factors Comput. Syst., 2018, p. 56.
- [28] E. Ohn-Bar, J. Guerreiro, D. Ahmetovic, K. M. Kitani, C. Asakawa, Modeling expertise in assistive navigation interfaces for blind people, in: Proc. Int. Conf. Intell. User Interfaces, 2018, pp. 403–407.
- [29] H.-S. Moon, J. Seo, Prediction of human trajectory following a haptic robotic guide using recurrent neural networks, in: Proc. IEEE World Haptics Conf., 2019, pp. 157–162.
- [30] F. Zhang, J. Leitner, M. Milford, B. Upcroft, P. Corke, Towards vision-based deep reinforcement learning for robotic motion control, arXiv:1511.03791 (2015).
- [31] S. Bohez, T. Verbelen, E. De Coninck, B. Vankeirsbilck, P. Simoens, B. Dhoedt, Sensor fusion for robot control through deep reinforcement learning, in: Proc. IEEE/RSJ Int. Conf. Intell. Robot. Syst., 2017, pp. 2365–2370.
- [32] S. Gu, E. Holly, T. Lillicrap, S. Levine, Deep reinforcement learning for robotic manipulation with asynchronous off-policy updates, in: Proc. IEEE Int. Conf. Robot. Autom., 2017, pp. 3389–3396.
- [33] A. Martínez-Tenor, J. A. Fernández-Madrigal, A. Cruz-Martín, J. González-Jiménez, Towards a common implementation of reinforcement learning for multiple robotic tasks, Expert Syst. Appl. 100 (2018) 246–259.
- [34] I. Carlucho, M. De Paula, G. G. Acosta, Double q-pid algorithm for mobile robot control, Expert Syst. Appl. 137 (2019) 292–307.
- [35] Y. Chebotar, A. Handa, V. Makoviychuk, M. Macklin, J. Issac, N. Ratliff, D. Fox, Closing the sim-to-real loop: Adapting simulation randomization with real world experience, in: Proc. IEEE Int. Conf. Robot. Autom., 2019, pp. 8973–8979.
- [36] J. Tan, T. Zhang, E. Coumans, A. Iscen, Y. Bai, D. Hafner, S. Bohez, V. Vanhoucke, Sim-to-real: Learning agile locomotion for quadruped robots, arXiv:1804.10332 (2018).

- [37] T. Salimans, J. Ho, X. Chen, S. Sidor, I. Sutskever, Evolution strategies as a scalable alternative to reinforcement learning, arXiv:1703.03864 (2017).
- [38] N. Hansen, The cma evolution strategy: a comparing review, in: Towards a New Evolutionary Computation, Springer, 2006, pp. 75–102.
- [39] N. Shafii, N. Lau, L. P. Reis, Learning to walk fast: Optimized hip height movement for simulated and real humanoid robots, J. Intell. Robot. Syst. 80 (3-4) (2015) 555–571.
- [40] C. Gehring, S. Coros, M. Hutler, C. D. Bellicoso, H. Heijnen, R. Diethelm, M. Bloesch, P. Fankhauser, J. Hwangbo, M. Hoepflinger, et al., Practice makes perfect: An optimization-based approach to controlling agile motions for a quadruped robot, IEEE Robot. Autom. Mag. 23 (1) (2016) 34–43.
- [41] T. Josh, F. Rachel, R. Alex, S. Jonas, Z. Wojciech, A. Pieter, Domain randomization for transferring deep neural networks from simulation to the real world, in: Proc. IEEE/RSJ Int. Conf. Intell. Robot. Syst., 2017, pp. 23–30.
- [42] T. Lei, G. Paolo, M. Liu, Virtual-to-real deep reinforcement learning: Continuous control of mobile robots for mapless navigation, in: Proc. IEEE/RSJ Int. Conf. Intell. Robot. Syst., 2017, pp. 31–36.
- [43] A. H. Qureshi, Y. Nakamura, Y. Yoshikawa, H. Ishiguro, Robot gains social intelligence through multimodal deep reinforcement learning, in: Proc. IEEE-RAS Int. Conf. Humanoid Robots, 2016, pp. 745–751.
- [44] A. Ghadirzadeh, J. Bütepage, A. Maki, D. Kragic, M. Björkman, A sensorimotor reinforcement learning framework for physical human-robot interaction, in: Proc. IEEE/RSJ Int. Conf. Intell. Robot. Syst., 2016, pp. 2682–2688.
- [45] D. Ha, J. Schmidhuber, World models, arXiv:1803.10122 (2018).
- [46] D. P. Kingma, M. Welling, Auto-encoding variational bayes, arXiv:1312.6114 (2013).

- [47] S. Hochreiter, J. Schmidhuber, Long short-term memory, Neural Comput. 9 (8) (1997) 1735–1780.
- [48] H.-S. Moon, J. Seo, Observation of human response to a robotic guide using a variational autoencoder, in: Proc. IEEE Int. Conf. Robot. Comput., 2019, pp. 258–261.
- [49] S. Balasubramanian, A. Melendez-Calderon, E. Burdet, A robust and sensitive metric for quantifying movement smoothness, IEEE Trans. Biomed. Eng. 59 (8) (2011) 2126–2136.
- [50] A. Nguyen, D. Kanoulas, L. Muratore, D. G. Caldwell, N. G. Tsagarakis, Translating videos to commands for robotic manipulation with deep recurrent neural networks, in: Proc. IEEE Int. Conf. Robot. Autom., 2018, pp. 1–9.
- [51] S. Balasubramanian, A. Melendez-Calderon, A. Roby-Brami, E. Burdet, On the analysis of movement smoothness, J. Neuroeng. Rehabil. 12 (1) (2015) 112.
- [52] C. M. Harris, D. M. Wolpert, Signal-dependent noise determines motor planning, Nature 394 (6695) (1998) 780–784.
- [53] D. A. Winter, Human balance and posture control during standing and walking, Gait & posture 3 (4) (1995) 193–214.